POTENTIAL FIELDS NAVIGATION OF LIFEGUARD ASSISTANT ROBOT FOR MASS MARINE CASUALTY RESPONSE

An Undergraduate Research Scholars Thesis

by

REBECCA THIER SCHOFIELD

Submitted to the Undergraduate Research Scholars program at
Texas A&M University
in partial fulfillment of the requirements for the designation as an

UNDERGRADUATE RESEARCH SCHOLAR

Approved by Research Advisor: Dr. Robin R. Murphy

May 2018

Major: Computer Science

TABLE OF CONTENTS

ABSTRACT

Potential Fields Navigation of Lifeguard Assistant Robot for Mass Marine Casualty Response

Rebecca Thier Schofield
Department of Computer Science and Engineering
Texas A&M University

Research Advisor: Dr. Robin R. Murphy
Department of Computer Science and Engineering
Texas A&M University

This thesis creates and implements an algorithm to enable the commercially available Emergency Integrated Lifesaving Lanyard (EMILY) lifeguard assistant robot boat to autonomously move towards marine victims. To achieve this, an attractive artificial potential field with GPS input was implemented.

Currently, lifeguards working to save Syrian refugees crossing into Greece teleoperate EMILY to people in the water, but due to restricted depth perception, often overshoot and collide with the victim.

The research benefits the safety, security, and rescue robotics research community. In addition, there are two societal benefits. One is that if EMILY can autonomously refine its navigation towards those in the water, the victims have a higher likelihood of quick rescue. Second, is that it would free the lifeguard to rescue victims in higher states of distress while the robot autonomously navigated to less vulnerable victims. Risks include the difficulty of data collection in open water, due to weather conditions.

The system was demonstrated at a two locations: 12 runs at a pond in John Crompton Park and 7 runs at Lake Bryan. Trials were conducted at a range of 30 meters at the pond and a range of 100 meters at the lake. During the close range experiments, the magnitude profile implemented on the artificial potential field was varied between a constant profile, a linear profile, and an exponential profile. Each profile was tested from all four quadrants surrounding the goal. During the far range experiments, the magnitude profile was again varied, with the addition of different exponential profile. The goal radius was also varied in these trials, between 2 meters and 1 meter from the goal point.

The velocity profile of each run was then examined. Ideal behavior is fast operation farther away from the target and slow operation near the target. Therefore the ideal velocity profile would have a steadily decreasing speed as the distance to the goal decreased. In both the close and far range trials applying an exponential magnitude profile to the artificial potential field implementation showed a roughly linear decrease in velocity as EMILY approached the goal- displaying the desired behavior.

DEDICATION

To Herb and Marlene Thier, for a lifetime of support and gentle encouragement to pursue scientific research.

ACKNOWLEDGMENTS

First, I would like to thank my advisor, Dr. Robin Murphy. Thank you for all the guidance and instruction you have given me. From the day I started at Texas A&M you have held me to higher standards than I knew I was capable of achieving. Thank you for being a role model to me. I also want to acknowledge my labmates, for their advice and help with this work. Grant Wilde, thank you. I would not have completed this thesis without your mentorship. Xuesu Xiao, Jan Dufek, Katerina Boyer, and Chinaemere Ike, thank you for your help with development and data collection.

I am immeasurably lucky to have a substantial support system of friends and family. I would not be where I am today without my parents. I would not have as much daily laughter without my brother, Ricky. I have far too many wonderfully supportive friends to list here. Thank you all for being in my life, but especially to Katherine and Tim for your help on this thesis.

NOMENCLATURE

CRASAR	Center for Robot-Assisted Search and Rescue
EMILY	Emergency Integrated Lifesaving Lanyard
GPS	Global Positioning System
PWM	Pulse Width Modulation
TEES	Texas A&M Engineering Experiment Station
USV	Unmanned Surface Vehicle

LIST OF FIGURES

FIGURE Page

LIST OF TABLES

TABLE Page

1. INTRODUCTION

Water rescue is a difficult task. Lifeguards must adapt to their particular area's currents and landscape, and much of the response hinges on quick recognition of persons in trouble. When conditions are particularly challenging, it is even more difficult to retrieve an individual from the water safely. In the case of the European refugee crisis, responders must perform mass rescues in often rough conditions. The worst tragedy in 2015, on record at the International Organization for Migration, occurred when a boat carrying approximately 800 migrants capsized off the coast of Italy, and only 28 could be rescued in time [2]. There is a great need to assist responders in these difficult situations.

Prior work by the TEES Center for Robot-Assisted Search and Rescue has used the commercially available Emergency Integrated Lifesaving Lanyard (EMILY) to assist the Hellenic Coast Guard, Hellenic Red Cross, and other lifeguards with refugees crossing from Turkey into Greece [3]. EMILY is a radio-controlled miniature jet ski covered with flotation and handles permitting up to 5 victims to hang on. Under funding from the National Science Foundation, CRASAR will assist both Greece and the Italian Coast Guard in rescuing people in the water.

This project is motivated by the need to for EMILY to reach victims in the water quickly, but also at an appropriate speed. If EMILY is moving too quickly, it could strike the victim and injure them further. However in a mass marine casualty, quick rescue of drowning victims is crucial. A navigation system with decreasing speed relative to the distance to the victim is needed. This system must be autonomous in order to keep a responder free to save other victims.

This project implements an artificial potential field to navigate EMILY autonomously to a GPS location and examines the performance of different magnitude profiles to de-

crease speed as EMILY approaches the goal location.

2. LITERATURE REVIEW

In a marine search and rescue scenario, any human or cluster of humans in the water must be reached effectively and without further injury. EMILY must be able to identify and approach them. The most promising method of solving these problems for this is to use GPS to direct EMILY to the desired location.

Approaches considered will be related to the approach of humans in open water with an unmanned surface vehicle. Other work with GPS and potential fields was examined in order to determine appropriate methods and metrics.

2.1 Methods of Marine Victim Approach

Many methods of navigating a unmanned surface vehicle to a waypoint in open water are in use. Several papers use methods like path planning in advance with a mathematical model [4][5] and probabilistic model checking [6], but require planning in advance. A more general, reactive approach is required. A route planning method based on a combination of an artificial potential field and A* search was proposed in simulation [7]. This did not consider humans, but showed use of a repulsive potential field for obstacle avoidance.

Work with humans often represents humans as GPS waypoints when considering this problem [8][9], the latter using thermal detection when close to a human victim for verification of rescue. A paper from the ICARUS project similarly represented a potential human victim with GPS and used PID control for navigation of the USV [10].

2.2 Experimental Metrics of Marine Victim Approach

Existing experimental metrics for testing the GPS approach of human victims in open water were found to measure a detection of a human victim [9], the reaching of a human victim [10], and the speed of the boat during the approach [10]. Experiments in [10] were

conducted over eight days of field exercises in open water, only one experimental run was conducted for [9].

2.3 Experimental Metrics of Artificial Potential Fields

Literature using artificial potential fields for path planning showed experimental metrics of path distance and time [11] as well as the maximum and average speed of the robot throughout the run [12].

2.4 Discussion

A GPS waypoint can quickly represent a human or cluster of humans [7][5][10] and PID control can be used to direct a robot to this waypoint [10]. The average speed can be used to evaluate the performance of an experimental run [12].

3. APPROACH

This chapter will discuss the theoretical approach of this potential fields implementation and the parameters used.

3.1 Theory of Potential Fields

An artificial potential field is a field of vectors representing the motor action of an agent [13]. Each vector has a magnitude and a theta component representing the desired movement of the agent. The agent calculates the appropriate vector at each timestep.

An attractive potential field was used for this work. This potential field represents the goal point as desirable, with all vectors in the field pointing towards it.

3.2 Potential Fields Implementation

The percepts used here for generation of the attractive potential field are the GPS coordinates and heading of the agent. The GPS coordinates of the victim are used for the goal point.

A magnitude profile is how the magnitude calculation changes based on the agent's current distance to the goal point. This distance is compared to the control region radius, a distance at which the field is in effect for the robot. Several magnitude profiles can be used, the ones examined in this work are: constant, linear, and exponential with two different powers.

If at any point the distance from the agent to the goal point is larger than the control region radius, the field is not in effect and the magnitude of the control vector is 0.

When the agent is less than a particular distance away from the goal point, the goal radius, the magnitude of the control vector is also 0 and the operation terminates.

3.3 Magnitude Calculation

The calculation for the magnitude component with each magnitude profile is presented below. Calculated magnitude is between 0 and 1, by convention [13] and to later allow for translation to agent-specific values. The distance from goal parameter is calculated as the distance between the agent's current GPS location and the goal GPS location.

3.3.1 Constant Magnitude Profile

A constant profile returns a constant magnitude C while the field is in effect, regardless of the agent's distance from the goal point. In this work, C is set to 1.

$$V_{magnitude} = C \tag{3.1}$$

3.3.2 Linear Magnitude Profile

A linear profile allows for a steady decrease in magnitude, depending on how close the agent is to the goal.

$$V_{magnitude} = \frac{distance\_from\_goal}{control\_region\_radius} \tag{3.2}$$

3.3.3 Exponential Magnitude Profiles

An exponential profile decreases the magnitude exponentially. Two exponential profiles were examined, with one squaring the linear magnitude and another taking it to the fourth power.

$$V_{magnitude} = (\frac{distance\_from\_goal}{control\_region\_radius})^2 \tag{3.3}$$

$$V_{magnitude} = (\frac{distance\_from\_goal}{control\_region\_radius})^4 \tag{3.4}$$

3.4 Theta Calculation

In this work, the theta component is calculated in terms of GPS heading. The target heading parameter is the bearing between the agent's current GPS position and the goal GPS position.

$$V_{theta} = target\_heading - current\_heading \tag{3.5}$$

4. IMPLEMENTATION

This chapter will discuss the adaptation of the theoretical algorithm described in the previous chapter to usage with EMILY and the integration into the existing system.

EMILY (seen below in Figure 4.1) is a commercially available mini-set ski USV. It measures 1.2 m long and 0.3 m wide and weighs 11 kg, with a top speed of 13.41 m/s. The specific EMILY used in this work has been modified by the group for autonomous use. An onboard Pixhawk Mini is used for control.

Figure 4.1: Photo of EMILY, reprinted from [1]

Code was developed in Python 3 running on a Raspberry Pi 3 onboard EMILY. The

Raspberry Pi was connected to EMILY's Pixhawk. The developed script connected to the Pixhawk over Mavproxy, through a Wi-Fi network both could connect to in the field. Control in the script was done in a while loop with a 0.075 second delay between iterations.

4.1 Magnitude Implementation

To calculate $V_{magnitude}$ for EMILY, the distance from the goal is required. This is calculated as the distance between the current GPS position of EMILY (read from the Pixhawk) and the goal GPS position. This distance is calculated with the Haversine formula, in meters. The code for this calculation is shown in Figure 4.2.

```
# returns in meters
def dist_between_gps_pts(lat1_deg, lon1_deg, lat2_deg, lon2_deg):
    # convert decimal degrees to radians
    lat1_rad = radians(lat1_deg)
    lon1_rad = radians(lon1_deg)
    lat2_rad = radians(lat2_deg)
    lon2_rad = radians(lon2_deg)

    # haversine formula
    dlat = lat2_rad - lat1_rad
    dlon = lon2_rad - lon1_rad
    a = sin(dlat/2)**2 + cos(lat1_rad) * cos(lat2_rad) * sin(dlon
   /2)**2
    c = 2 * asin(sqrt(a))

    # radius of earth in meters
    R = 6371000

    return c * R
```

Figure 4.2: Code for distance_from_goal calculation

This calculated distance from the goal is then used in one of the magnitude profiles, in Equations 3.1 - 3.4.

4.2 Theta Implementation

To calculate $V_{direction}$ for EMILY, the current heading and target heading are required. The current heading is read from the Pixhawk. The target heading is calculated from the current and goal GPS points. The code for this calculation is shown in Figure 4.3.

Two adjustments must be made to the calculated bearing to achieve a target heading that matches EMILY's reference frame. First, the calculation is scaled to the range [0, 360). Next, 90 degrees is subtracted from the measurement, to adjust the true north reference to the x-axis reference used by the Pixhawk. Finally, the calculation is scaled again to the range of [0, 360).

```
# returns in degrees
def get_bearing(lat1_deg, lon1_deg, lat2_deg, lon2_deg):
    # convert decimal degrees to radians
    lat1_rad = radians(lat1_deg)
    lon1_rad = radians(lon1_deg)
    lat2_rad = radians(lat2_deg)
    lon2_rad = radians(lon2_deg)

    dy = lat2_rad - lat1_rad
    dx = cos(pi/180*lat1_rad)*(lon2_rad - lon1_rad)
    angle = atan2(dy, dx);

    theta = 360 - (degrees(angle) % 360)

    # subtracting 90 degrees to sync up true north and x axis = 0
    theta = (theta + 90) % 360

    return theta
```

Figure 4.3: Code for target_heading calculation

This calculated target heading is then used in Equation 3.5.

4.3 Integration with EMILY

The method above calculates V at any given timestep, with magnitude and theta components. In order to translate V to motion on EMILY, these components were transformed into commands that the EMILY can understand. This is done by converting to PWM values and sending to the Pixhawk controller in EMILY. $V_{magnitude}$ is used to compute a PWM value for thrust, and V_{theta} is converted to a PWM value for the rudder. The thrust PWM value ranges from 1500 (no movement) to 1900 (full speed). In this work, the highest thrust PWM value possible for the potential field is set to 1750. The rudder PWM value ranges from 1100 (hard left turn) to 1900 (hard right turn). The full range for the rudder PWM values is used here.

The magnitude and theta values are first scaled by constant values before this translation to PWM.

$$scaled\_magnitude = V_{magnitude} \times \alpha_{magnitude} \tag{4.1}$$

$$scaled\_theta = V_{theta} \times \alpha_{direction} \tag{4.2}$$

These constant values are implemented as tuning parameters and were determined with field testing during development and shown in Equations 4.3 and 4.4.

$$\alpha_{magnitude} = 5 \tag{4.3}$$

$$\alpha_{direction} = 1.75 \tag{4.4}$$

For translation of magnitude and theta values to the thrust and rudder values required, two methods were used: proportional scaling and a 'turning mode', a method used here [14]. The method used depends on the value of the initial theta component. If this value

is within a set 'angle window', the proportional scaling method is used. If not, the turning mode turns EMILY in place. For either mode, the PWM values calculated are rounded down to a multiple of 5 and any values outside the acceptable range are corrected before being sent to the Pixhawk.

4.3.1 Proportional Scaling

In this mode, theta is within the set angle window. The magnitude and theta values are scaled to thrust and rudder PWM values, within the ranges of [1500, 1750] and [1100, 1900] respectively.

$$scale\_thrust = PWM\_thrust\_range\_max - PWM\_thrust\_range\_min \quad (4.5)$$

$$Thrust\_PWM = scaled\_magnitude \times scale\_thrust + PWM\_thrust\_range\_min \quad (4.6)$$

$$scale\_rudder = PWM\_turning\_range\_max - PWM\_turning\_range\_min \quad (4.7)$$

$$Rudder\_PWM = \frac{scaled\_theta - (-180)}{(180) - (-180)} \times scale\_rudder + PWM\_turning\_range\_min \quad (4.8)$$

4.3.2 Turning Mode

When theta is outside of the angle window, EMILY will be set at a low constant speed (the PWM value used here is 1580) and the rudder will turn sharply until the current heading is within the window. The angle window for this work was set to 45 degrees, based on tuning in the field.

$$Thrust\_PWM = 1580 \tag{4.9}$$

$$Rudder\_PWM = \begin{cases} PWM\_turning\_range\_min, & \text{if } theta < -angle\_window \\ PWM\_turning\_range\_max, & \text{if } theta > angle\_window \end{cases} \tag{4.10}$$

5. DEMONSTRATIONS

The following chapter will discuss the methods used for demonstrating this system. The system was tested both at close range, in four quadrants, and at a far range. Close range was selected at 30 meters and far range was selected at 100 meters. 12 runs were conducted at close range and 7 runs at far range.

Operation at this far range, which is a realistic operating range for EMILY, will show velocity measurements and profiles when EMILY is started far from the victim. Demonstrating operation at this close range will show results for a case if EMILY is launched near the victim. A velocity profile that shows ideal behavior (decreasing while approaching the victim) in both cases is preferred, in order to account for a variable starting distance of EMILY from a victim.

Both the close range and far range data collection resulted in velocity profiles where the exponential magnitude profile taken to the second power was shown to exhibit the desired behavior of EMILY speed during a run. These results and ideal behaviors are described further in Chapter 6.

5.1 Close Range Data Collection

For close range runs, the system was tested in the pond at John Crompton Park in College Station, TX. These tests provided a verification of the system from multiple angles. The control region radius parameter was set to 30 meters. The wind conditions were noted as 2.7 mph from the western direction, from the Weather Channel mobile application. An example of a path taken during this data collection is shown in Figure 5.1, where the starting point is at the bottom right of the path shown and the goal point is at the top left.

The goal point was placed roughly in the middle of the pond, to allow for maximum operation in the area. EMILY was driven to a central location and the GPS position was

Figure 5.1: .kml file taken at close range during run with exponential profile in Q3

noted. All operation was filmed with a Samsung Galaxy S6.

12 runs were conducted, with 3 magnitude profiles (constant, linear, and an exponential profile) in each of the 4 quadrants (denoted as Q1, Q2, Q3, and Q4) surrounding the goal. Before a run, EMILY was driven by an operator to a quadrant. The potential field was then initialized with the appropriate magnitude profile. Operation terminated normally if

EMILY was at any point 2 meters or closer to the goal point, this was set as the goal radius.

Each GPS coordinate, heading, and distance to the goal was recorded in the log files. This data was used to compute the results in the following chapter.

5.2 Far Range Data Collection

Far range trials were conducted at Lake Bryan in Bryan, TX. This showed operation at a greater range, closer to the realistic operating range of EMILY, from just one angle. The water conditions were different from the pond, where this was open water. The control region radius parameter was set to 100 meters. The wind conditions were noted as 13 mph from the north/northeastern direction, from the Weather Channel mobile application. This wind was moving in an opposite direction to the movement of EMILY and noticeably impacted operation. The velocity calculations are likely significantly affected by the wind speed and direction during the runs.

An exponential profile, taken to a factor of 4 instead of 2, was added during these demonstrations to further examine the behavior of the overall exponential profile. Additionally, the goal radius parameter was varied, trials were conducted with a goal radius of 2 meters and of 1 meter.An example of a path taken during this data collection is shown in Figure 5.2, where the starting point is at the bottom of the path shown and the goal point is at the top.

The goal point was determined by finding a point 100 meters from the initial launch site at a 315 degree bearing. This point was found with a laser range finder. All operation was filmed with an external GoPro camera.

8 runs were conducted, with 4 magnitude profiles (constant, linear, and two exponential profiles) and 2 different goal radii (1 meter and 2 meters). Before a run, EMILY was driven by an operator to a point near the initial launch site and pointed to the quadrant of the goal point. The potential field was then initialized with the appropriate magnitude profile and

Figure 5.2: .kml file taken at far range during run with exponential profile to the second power with a termination radius of 2

goal radius. Operation terminated normally if EMILY was closer to the goal point than the set goal radius.

The final run, with the combination of the exponential profile to the fourth power and the goal radius of 1 meter, was aborted when wind blew over the long range Wi-Fi antenna and broke it. This prematurely ended the far range demonstrations.

Each GPS coordinate, heading, and distance to the goal was recorded in the log files. This data was used to compute the results in the following chapter.

6. RESULTS

This chapter presents the results from the close range and the far range demonstrations. The behaviors resulting from the combinations of parameters demonstrated will be examined and compared to an ideal behavior.

The ideal behavior is of a high velocity further from the goal and a lower velocity close to the goal. This is desired so EMILY operates at a fast speed when farther away from the victim and operates at a slow speed when near the victim. This behavior allows for EMILY to both move quickly for a fast rescue and to avoid high speeds when close to a victim- which could injure them further if struck by EMILY.

6.1 Close Range Results

6.1.1 Average Velocity

The average velocity for the run was calculated by dividing the total distance traveled by EMILY (meters) by the total running time (seconds). These results are shown in Table 6.1.

6.1.2 Velocity At Termination

The velocity at termination is calculated from the change in distance over the final second of the run. The distance measured at which EMILY received the final command is also provided, read from the log files as the last distance tracked. The distance results are shown in Table 6.2 and the velocity upon termination results are shown in Table 6.3.

6.1.3 Velocity Profiles

Graphs of each velocity profile, calculated velocity at each time step plotted against the distance of EMILY from the goal point, are presented here, in Figures 6.1 - 6.4.

Table 6.1: Average velocity of each run at close range

Trial	Magnitude Profile	Quadrant	Velocity (m/s)
1	Constant	1	1.3573
2	Linear	1	1.3457
3	Exponential (squared)	1	1.8253
4	Constant	2	2.0147
5	Linear	2	2.3616
6	Exponential (squared)	2	1.753
7	Constant	3	2.8873
8	Linear	3	2.1155
9	Exponential (squared)	3	1.513
10	Constant	4	2.0474
11	Linear	4	1.746
12	Exponential (squared)	4	1.5675

Table 6.2: Termination distance of each run at close range

Trial	Magnitude Profile	Quadrant	Termination Distance (m)
1	Constant	1	2.1136
2	Linear	1	2.5054
3	Exponential (squared)	1	2.1534
4	Constant	2	2.5230
5	Linear	2	2.1499
6	Exponential (squared)	2	2.0255
7	Constant	3	2.3799
8	Linear	3	2.3562
9	Exponential (squared)	3	2.0126
10	Constant	4	2.8085
11	Linear	4	2.0990
12	Exponential (squared)	4	2.0756

6.2 Close Range Analysis

In three of the four quadrants in the close range tests, the average velocity of the runs was evenly spaced between the different profiles. In the remaining quadrant, Q1, the

Table 6.3: Velocity upon termination of each run at close range

Trial	Magnitude Profile	Quadrant	Velocity On Termination (m/s)
1	Constant	1	1.4775
2	Linear	1	1.1597
3	Exponential (squared)	1	1.0694
4	Constant	2	2.9793
5	Linear	2	2.8796
6	Exponential (squared)	2	1.0976
7	Constant	3	3.5800
8	Linear	3	2.6563
9	Exponential (squared)	3	0.9576
10	Constant	4	3.0761
11	Linear	4	3.3856
12	Exponential (squared)	4	0.7866

average speed for the constant profile measured very close to the average speed for the linear profile. The percent differences between average velocity measurements are shown in Table 6.4.

Table 6.4: Percent difference of average velocity measurements at close range

Quadrant	Magnitude Profiles	Percent Difference (%)
1	Constant and Linear	0.85
1	Linear and Exponential (squared)	26.28
2	Linear and Constant	14.69
2	Constant and Exponential (squared)	14.93
3	Constant and Linear	36.48
3	Linear and Exponential (squared)	28.48
4	Constant and Linear	17.26
4	Linear and Exponential (squared)	10.22

For Q3 and Q4, the constant profile had the greatest average speed. In Q1 and Q2, the

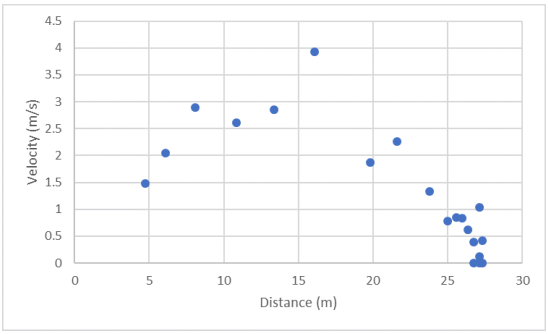

(a) Constant Profile

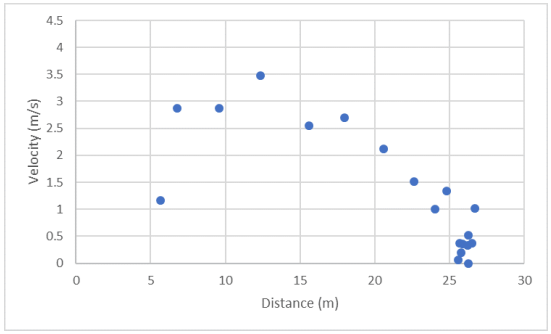

(b) Linear Profile

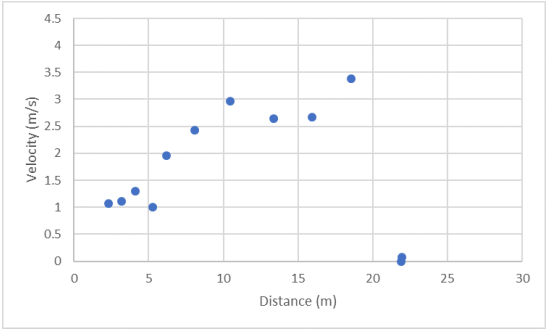

(c) Exponential (squared) Profile

Figure 6.1: Velocity profiles presented for runs in quadrant 1

linear profile had the greatest average speed. During operation in all four quadrants, the exponential profile resulted in the least average speed.

In all quadrants, the exponential profile had the lowest velocity upon termination. In every quadrant but Q4, the constant profile had the greatest velocity after termination. These results match with the expected ones, except for the performance of the constant profile in Q4.

The velocity profiles, presented in Figures 6.1 - 6.4, echo these results. The graphs for linear profile in each quadrant more closely resembles the corresponding constant profile than the exponential profile. The linear decrease in the magnitude calculation was not reflected in the velocity profile. The exponential profile reduces speed further out from the

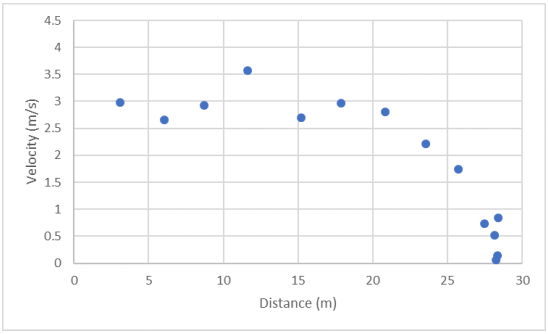

(a) Constant Profile

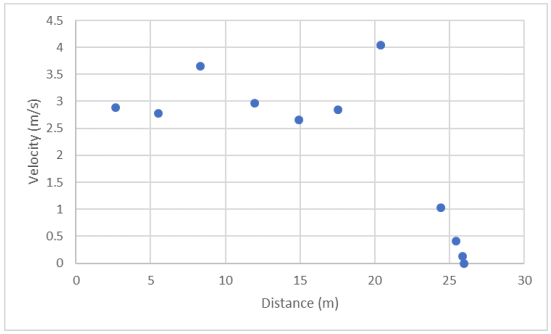

(b) Linear Profile

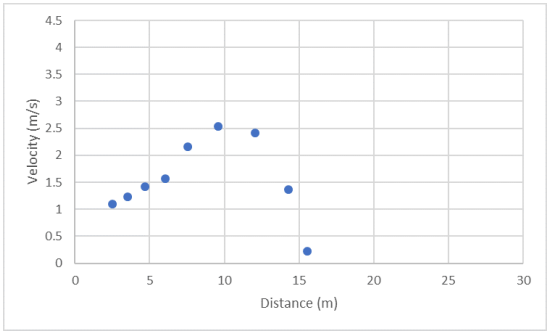

(c) Exponential (squared) Profile

Figure 6.2: Velocity profiles presented for runs in quadrant 2

goal point, but this results in a slower overall approach of the goal.

Both the linear and the exponential profiles show the ideal behavior in the close range demonstrations. However, the exponential profile for each quadrant shows a roughly linear decrease in speed near the goal. The exponential profile applied to the magnitude in the artificial potential field, in the close range demonstrations, is nearest to the ideal behavior desired.

These close range trials were conducted in a small pond, where 30 meters was the maximum achievable operating range. EMILY was able to complete these short runs quickly, with no run exceeding an operation time of 20 seconds. Because of this, the velocity data collected is limited. The collection of more data points, either with repeated trials

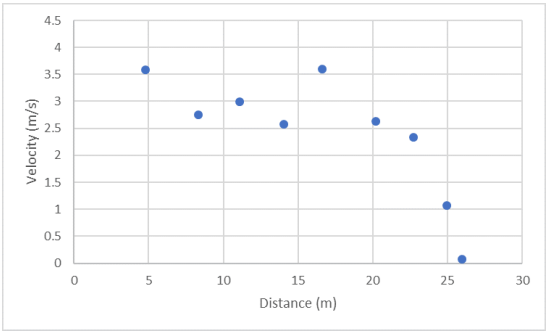

(a) Constant Profile

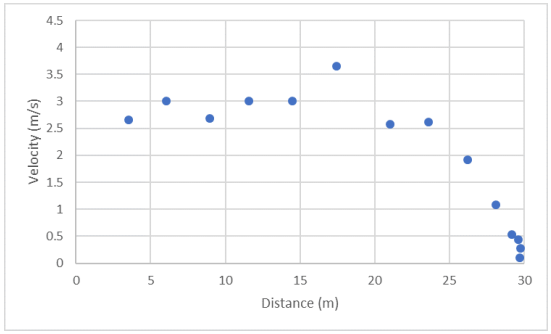

(b) Linear Profile

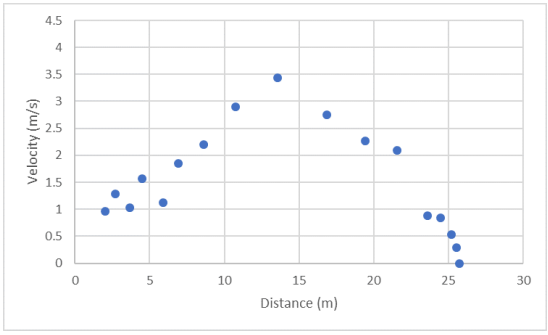

(c) Exponential (squared) Profile

Figure 6.3: Velocity profiles presented for runs in quadrant 3

across all 4 quadrants or with a slightly larger maximum operating range, would have more clearly shown the trends of the velocity profiles.

6.3 Far Range Results

6.3.1 Average Velocity

The average velocity for the run was calculated by dividing the total distance traveled by EMILY (meters) by the total running time (seconds). These results are shown in Table 6.5.

6.3.2 Velocity At Termination

The velocity at termination is calculated from the change in distance over the final second of the run. The distance measured at which EMILY received the final command is

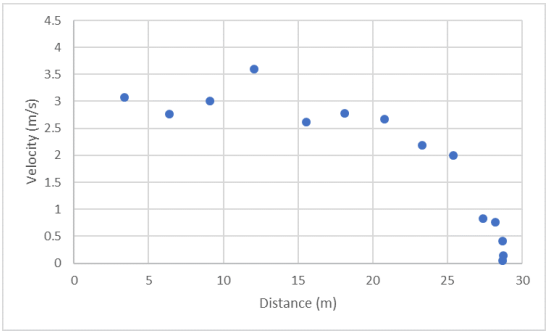

(a) Constant Profile

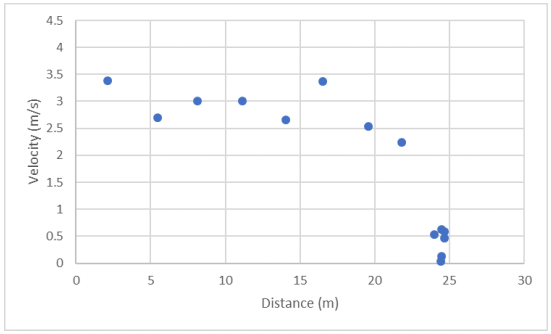

(b) Linear Profile

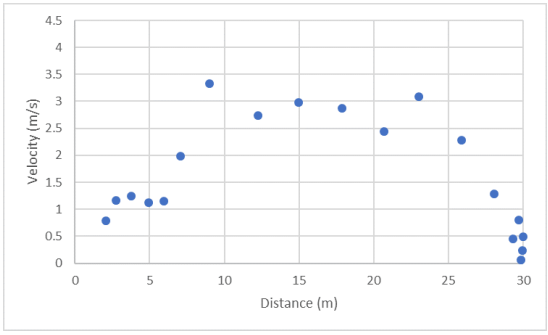

(c) Exponential (squared) Profile

Figure 6.4: Velocity profiles presented for runs in quadrant 4

Table 6.5: Average velocity of each run at far range

Trial	Magnitude Profile	Goal Radius (m)	Velocity (m/s)
1	Constant	2	1.8627
2	Linear	2	1.5051
3	Exponential (squared)	2	0.7887
4	Exponential (fourth)	2	0.693
5	Constant	1	1.4428
6	Linear	1	1.5119
7	Exponential (squared)	1	0.9306
8	Exponential (fourth)	1	Aborted

also provided, read from the log files as the last distance tracked. The distance results are shown in Table 6.6 and the velocity upon termination results are shown in Table 6.7.

Table 6.6: Termination distance of each run at far range

Trial	Magnitude Profile	Goal Radius (m)	Termination Distance (m)
1	Constant	2	2.0186
2	Linear	2	2.0410
3	Exponential (squared)	2	2.0216
4	Exponential (fourth)	2	2.0282
5	Constant	1	1.0906
6	Linear	1	1.2049
7	Exponential (squared)	1	1.0030
8	Exponential (fourth)	1	Aborted

Table 6.7: Velocity upon termination of each run at far range

Trial	Magnitude Profile	Goal Radius (m)	Velocity On Termination (m/s)
1	Constant	2	1.6430
2	Linear	2	1.0780
3	Exponential (squared)	2	0.2730
4	Exponential (fourth)	2	0.5119
5	Constant	1	0.7082
6	Linear	1	1.0363
7	Exponential (squared)	1	0.2985
8	Exponential (fourth)	1	Aborted

6.3.3 Velocity Profiles

Graphs of each velocity profile, calculated velocity at each time step plotted against the distance of EMILY from the goal point, are presented here, in Figures 6.6 and 6.7.

6.4 Far Range Analysis

When the goal radius was set to 2 meters, the constant profile performed the fastest and the exponential profile to the fourth power performed the slowest. However, the linear profile performed the fastest when the goal radius was 1 meter. For this radius, the expo-

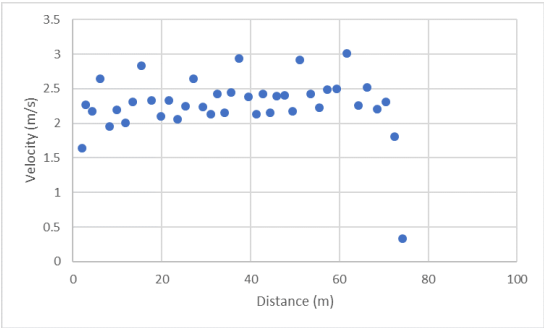

(a) Constant Profile

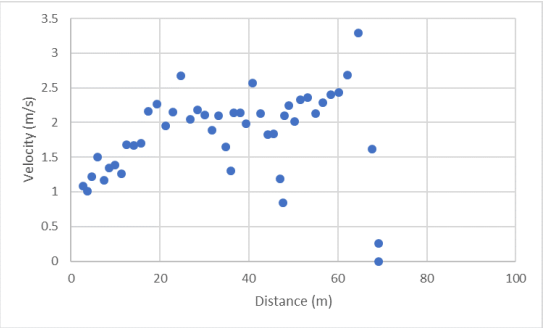

(b) Linear Profile

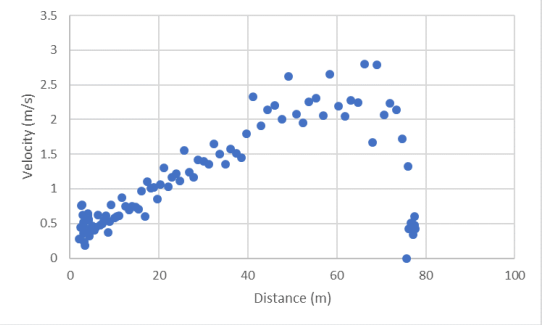

(c) Exponential (squared) Profile

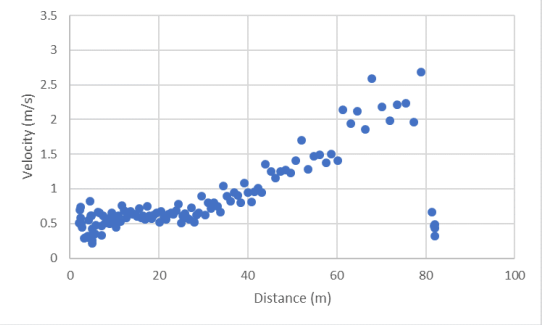

(d) Exponential (fourth) Profile

Figure 6.5: Velocity profiles presented for runs with a goal radius of 2 meters

nential profile to the second power performed the slowest, but the run testing the profile to the fourth power was aborted.

For both goal radii, the exponential profile to the second power had the slowest velocity on termination. The constant profile had the greatest termination velocity when the goal radius was set to 2 meters, but the linear profile had the greatest when the goal radius was set to 1 meter. There was little difference in the velocity on termination between the two goal radii.

The velocity profiles, presented in Figures 5.5 and 5.6, show the overall trend of velocity through each run. For both goal radii used, the exponential profile to the second power exhibits roughly linear behavior. The linear profile resembles the constant behav-

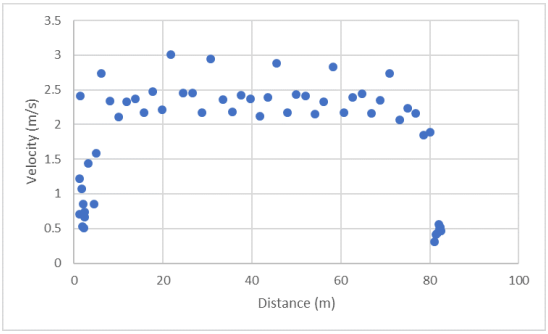

(a) Constant Profile

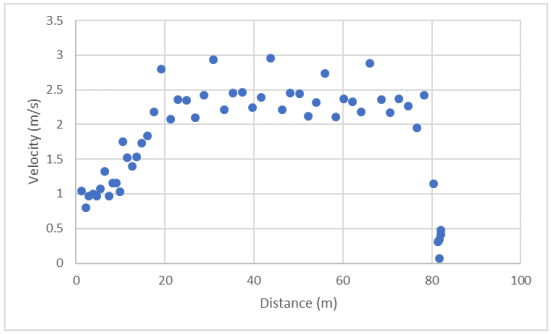

(b) Linear Profile

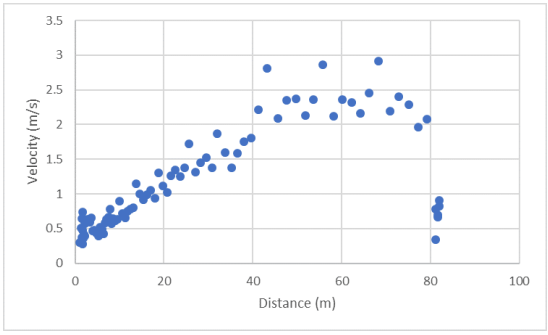

(c) Exponential (squared) Profile

Figure 6.6: Velocity profiles presented for runs with a goal radius of 1 meter

ior, more notably in the second set of trials (with the goal radius at 1 meter). In both sets, the exponential profile to the second power starts decreasing in speed sooner than the linear profile.

In these far range demonstrations, the trends in the velocity profiles are more clear due to the increased number of data points. The linear and both exponential profiles display the ideal behavior for EMILY. As was seen in the close range demonstrations, the exponential profile to the second power results in a roughly linear decrease in velocity as EMILY approaches the goal. The exponential profile to the fourth power resulted in a velocity profile that is more sensitive to the exponential relationship of the magnitude, with a change in velocity that resembles an exponential decrease. Both exponential profiles exhibit ideal

behavior.

These trials operated at a farther range than the previous trials thus allowing for more data to be gathered per run. However, the data collection was aborted prematurely. A strong gust of wind knocked over the long range Wi-Fi antenna used to connect the ground station with EMILY, and broke an internal wire. This prematurely ended the final run. Because of this termination, far range operation was only shown in one direction. The bearing from EMILY's starting position to the goal point was against the strong wind. This likely impacted the data collected. If 4 quadrant testing had been completed in this far range, the overall trends would have been visible regardless of direction relative to strong winds.

6.5 Overall Analysis

In both the close range and far range results, the implementation of an exponential magnitude profile, to the second power, shows a roughly linearly decreasing speed as the goal point is approached. When the additional exponential profile was added in the second set of trials, with the factor raised to the fourth power, it showed a behavior closer to an exponential decrease. Both a linear and an exponential decrease in speed match the ideal behavior. The results from both ranges support the application of an exponential magnitude profile to this potential fields implementation.

A key difference between the results from the two ranges is the behavior of the linear profile. At the farther distances, the linear magnitude profile results in a velocity that decreases linearly. This decrease occurs closer than the results of either exponential profile and results in a greater speed upon termination, but this does resemble the ideal behavior. However, when EMILY was started at closer distances, the linear magnitude profile did not appear to result in a similar decrease in speed. Instead, the velocity profile matched the profile resulting from the application of a constant profile to the potential fields. Because

the application of the linear profile only resulted in a velocity profile resembling the ideal behavior for the far range trials and not the close range trials, it is not the best selection to achieve the ideal behavior at a variety of starting distances.

7. CONCLUSIONS

This thesis presents a method for operating EMILY to a goal point in open water, using GPS as an input to an attractive potential field and mapping the vector generated in order to control EMILY. Several magnitude profiles were implemented and tested, along with two different goal radii. Demonstrations were conducted at a close range of 30 meters, from the four quadrants surrounding the goal point, and at a far range of 100 meters, in open water. Comparisons between the average velocity and velocity after the goal is reached showed that the constant profile often has the fastest average velocity during a run, but the exponential profile to the second power always had the slowest velocity upon termination. Both of these are the ideal traits for the application of quickly driving EMILY to a human victim out at sea, but slowing down enough to reach the victim without striking them. Examining the velocity profiles for each run indicates that the exponential profile to the second power has an approximately linear decrease in velocity upon approach of the victim. This graph behavior, combined with the lowest velocity on termination, indicates that an exponential magnitude profile applied to this potential fields implementation is ideal for use in future work as described below.

Future work would ideally examine the 4 quadrant performance at a far range, to see the performance at different headings. This work presents a limited set of far range trials, all of which operated in the same direction to the goal point. The direction of operation in these trials was against the direction of a 13 mph wind. Before other directions could be considered, the wind blew down the long range Wi-Fi antenna, breaking a wire when it fell on the ground. Further experiments run on another day, with either less wind or a more secured Wi-Fi antenna placement, would provide more data about the behavior of the velocity resulting from the applied magnitude profile. The close range data suggests

that the conclusions from the far range demonstrations (that an exponential profile shows the desired behavior) would still hold.

Finally, there is future work to improve EMILY's approach of a victim. GPS coordinates can contain error, or a victim can drift in water by the time EMILY reaches the previously set coordinates. An future addition to this work would be to add a reactive behavior that is given greater priority at a close range to the victim. A coordination of the two behaviors would function as the overall approach behavior, with the reactive behavior taking priority over the GPS-based behavior when an appropriate percept is present.

REFERENCES

[1] L. Silverman, "Meet emily, the lifeguard robot that's saving refugees crossing the mediterranean sea," *Kera News*.

[2] "Iom counts 3,771 migrant fatalities in mediterranean in 2015." Web, January 2016.

[3] R. Murphy, A. Mulligan, F. Boiteux, and J. Sims, "Cognitive work analysis of increasing the intelligence of a lifeguard assistant robot for mass marine casualty event," in *Association for the Advance of Artificial Intelligence Conference 2017*, in review.

[4] Z. Du, Y. Wen, C. Xiao, F. Zhang, L. Huang, and C. Zhou, "Motion planning for unmanned surface vehicle based on trajectory unit," *Ocean Engineering*, vol. 151, pp. 46–56, 2018.

[5] P. Tang, R. Zhang, D. Liu, L. Huang, G. Liu, and T. Deng, "Local reactive obstacle avoidance approach for high-speed unmanned surface vehicle," *Ocean Engineering*, vol. 106, pp. 128–140, 2015.

[6] D. Hermann, R. Galeazzi, J. C. Andersen, and M. Blanke, "Smart sensor based obstacle detection for high-speed unmanned surface vehicle," *IFAC-PapersOnLine*, vol. 48, no. 16, pp. 190–197, 2015.

[7] W. Chao, M. Feng, W. Qing, and W. Shuwu, "A situation awareness approach for usv based on artificial potential fields," in *2017 4th International Conference on Transportation Information and Safety (ICTIS)*, pp. 232–235.

[8] T. Tao and R. Jia, "Uav decision-making for maritime rescue based on bayesian network," in *Proceedings of 2012 2nd International Conference on Computer Science and Network Technology*, pp. 2068–2071.

[9] R. MendonÃğa, M. M. Marques, F. Marques, A. LourenÃğo, E. Pinto, P. Santana, F. Coito, V. Lobo, and J. Barata, "A cooperative multi-robot team for the surveillance of shipwreck survivors at sea," in *OCEANS 2016 MTS/IEEE Monterey*, pp. 1–6.

[10] A. Matos, E. Silva, N. Cruz, J. C. Alves, D. Almeida, M. Pinto, A. Martins, J. Almeida, and D. Machado, "Development of an unmanned capsule for large-scale maritime search and rescue," in *2013 OCEANS - San Diego*, pp. 1–8.

[11] G. Li, A. Yamashita, H. Asama, and Y. Tamura, "An efficient improved artificial potential field based regression search method for robot path planning," in *2012 IEEE International Conference on Mechatronics and Automation*, pp. 1227–1232, Aug 2012.

[12] G. Li, A. Yamashita, H. Asama, and Y. Tamura, "An efficient improved artificial potential field based regression search method for robot path planning," in *2012 IEEE International Conference on Mechatronics and Automation*, pp. 1227–1232, Aug 2012.

[13] R. R. Murphy, *Introduction to AI Robotics 2nd ed.* MIT Press, 2018.

[14] X. Xiao, J. Dufek, T. Woodbury, and R. Murphy, "Uav assisted usv visual navigation for marine mass casualty incident response," in *2017 IEEE/RSJ International Conference on Intelligent Robots and Systems (IROS)*, pp. 6105–6110, Sept 2017.